Polymer 50 (2009) 4618–4625

Contents lists available at ScienceDirect

Polymer

journal homepage: www.elsevier.com/locate/polymer

Acceleration effect of sericin on shear-induced β-transition of silk fibroin

Chang Seok Ki [a,c], In Chul Um [b], Young Hwan Park [a,c,*]

[a] Department of Biosystems and Biomaterials Science and Engineering, Seoul National University, Seoul 151-921, Republic of Korea
[b] Department of Natural Fiber Sciences, Kyungpook National University, Daegu 702-701, Republic of Korea
[c] Research Institute for Agriculture and Life Sciences, Seoul National University, Seoul 151-921, Republic of Korea

ARTICLE INFO

Article history:
Received 15 October 2008
Received in revised form
2 February 2009
Accepted 14 February 2009
Available online 24 February 2009

Keywords:
Fibroin
Sericin
β-Transition

ABSTRACT

Although silk sericin (SS) occupies 25% of silk protein, its importance has often been overlooked in the natural silk spinning process and in the formation of the crystalline structure of silk fibroin (SF). In this study, we elucidated the role of SS in the crystallization process of SF under shear using SF/SS blend solutions. In order to apply shear stress to the blend solution, a rotating glass rod was inserted into a glass tube filled with the solution and the shear rate was determined to be in the range of 598–724 s^{-1}. After shearing, SF aggregates were formed and the amount of the aggregates increased with shearing time. Additionally, it was observed that the aggregate formation and β-sheet transition of SF were enhanced when a proper amount of SS was in the blend solution. Consequently, the SS considerably contributes to the structural transition of SF under shear. The SS can improve the shear-induced β-sheet transition and crystallization of SF.

1. Introduction

Silk fiber, which is mainly composed of the proteins, fibroin and sericin, has been an excellent textile material for a long time due to its outstanding mechanical properties. Recently, silk protein has received much interest as a biomaterial for its biological compatibility and functionality. Accordingly, there have been many attempts to create silk-based materials for specific purposes through various fabrication methods, e.g., gelation, spinning, film casting and foaming [1–9]. Nevertheless, despite efforts of many researchers, the regenerated silk protein materials exhibit poor physical and mechanical properties compared with natural silk. This is probably due to a lack of understanding of the nature of silk protein itself and the spinning process of the silk worm.

Due to its stable β-sheet structure, silk fibroin (SF) has high crystallinity as well as high molecular orientation and provides excellent tensile strength as the main component of silk fiber. Therefore, most studies are mainly focused on formation of the well-developed β-sheet structure of SF. Subsequently, it was discovered that such structural characteristics originated from the unique nature of SF and were regulated by many complicated parameters. So far a number of studies have tried to elucidate these parameters and the results can be summarized as follows:

1. Repetition of a regular amino acid sequence
2. Concentration process of fibroin solution in gland and solidification
3. Shear stress in gland and drawing process

Among these determinants, shear stress is critical for SF to transition from a random coil conformation to a β-sheet structure in aqueous solution. It is generally accepted that SF molecules aggregate and crystallize by themselves under shear condition without methanol treatment [10–12].

Silk sericin (SS), which occupies 25% of total weight of raw silk fiber, is mostly removed by a degumming process because it is believed that sericin plays a limited adhesive role of binding two fibroin strands and raw fibers in cocoons. Very few have focused on the important role of sericin in the fiber formation process of silk and in the structural transition of SF. Hence, the SF structure in nature and the silk regeneration process have so far been studied exclusive of sericin. But in more recent studies, it was reported that the crystallization and the mechanical property of the regenerated silk could be affected by SS. Lee observed a retardation of recrystallization of SF in an SF/SS blend by methanol treatment, suggesting that there is physical interaction between SF and SS molecules due to hydrogen bonds [13]. Such an effect of SS may be due to SS' hydrophilicity and similar result has been reported that

* Corresponding author. Department of Biosystems and Biomaterials Science and Engineering, Seoul National University, Seoul 151-921, Republic of Korea. Tel.: +82 2 880 4622; fax: +82 2 873 2285.
E-mail address: nfhchempf@snu.ac.kr (Y.H. Park).

0032-3861/$ – see front matter © 2009 Published by Elsevier Ltd.
doi:10.1016/j.polymer.2009.02.017

the β-sheet transition of SF can be achieved by blending with hydrophilic polymer, such as hyaluronic acid, without any general crystallization process, methanol treatment or shearing [14]. We also found that the crystallinity and tensile strength of the regenerated silk filament, fabricated from partially degummed cocoons (containing ca. 10% SS), were improved [5]. These reports indicate that SS seems to play an important role in the structure and mechanical property of SF by affecting the conformational transition of SF molecules.

From our preliminary study, it was observed that the mechanical property of regenerated silk film cast from sheared SF/SS blend solutions was improved while the crystallinity and the mechanical property of SF/SS blend film prepared from unsheared solutions were hardly changed compared with those of pure SF film. And it was confirmed that the shear condition might play a key role in the β-sheet transition of SF in an SF/SS blend. Therefore, we discuss herein the role of sericin in the formation of SF crystalline structure in an SF/SS blend, focusing especially on the β-sheet transition.

2. Experimental section

2.1. Materials

In order to obtain pure SF, cocoons from *Bombyx mori* were boiled in an aqueous solution of 0.3% (w/v) sodium oleate and 0.2% (w/v) sodium carbonate for an hour and subsequently washed with warm distilled water several times, followed by drying at 60 °C. The degummed cocoons were then dissolved in 9.3 M LiBr aqueous solution for an hour at room temperature. The solution was filtered and dialyzed against distilled water using a cellulose tube (MWCO: 12–14 kDa) for 3 days. Then the aqueous SF solution was freeze-dried and eventually, the regenerated SF sponge was obtained. On the other hand, SS was extracted from the cocoons in 8 M urea solution for an hour at 80 °C. Then the solution was filtered and dialyzed following the same protocol as for SF solution. The SS solution was turned into a weak gel during the dialysis and finally the SS gel was freeze-dried.

The SF/SS blend solution was prepared by simultaneously dissolving the regenerated SF and SS at appropriate weight ratios in 9.3 M LiBr solution for an hour at room temperature. The mixing ratios of SF and SS were 100:0, 90:10, 80:20 and 75:25, and each sample was designated as SFSS1000, SFSS9010, SFSS8020 and SFSS7525, respectively. Then the completely dissolved SF/SS blend solution of 10% (w/v) was dialyzed for 3 days to remove salt. After the dialysis, the solutions of varying SF/SS blend ratios were diluted to concentrations in the range of 3–4.5 wt%. Hence, each solution was diluted or concentrated to the same concentration for measurements. To concentrate a solution, the dialyzed SF/SS solution was poured into a cellulose tube (MWCO: 3500 Da) and the tube was immersed in 50% (w/v) polyethylene glycol (M_w: 20,000) aqueous solution for appropriate times (approximately 8–12 h) at 4 °C to prevent denaturation by warm temperature or shearing.

The regeneration processes of SF and SS used in the experiments do not cause severe damage and hardly decrease the molecular weights [15–18]. Our preliminary study confirmed that the molecular weights of regenerated SF and extracted SS were not different from what has been reported when measured by electrophoresis (data not shown).

2.2. Shearing condition

For shearing, the concentrations of SF/SS blend solutions were adjusted to 5 wt% and each solution of 2 ml was moved into a glass which has an 11 mm inner diameter and 15 cm depth. Then a glass rod of 10 mm diameter was placed in the tube center. The length of the glass rod was 30 cm. The upper part was fixed on the spin motor's shaft and the opposite end located above 5 mm from the bottom of the glass tube. The gap between the tube wall and the rod was 0.5 mm. The glass rod was locked by a spin rate controllable motor and the spin rate was kept at 600 rpm (62.8 rad/s). In this condition, the shear rate was calculated by Eq. (1) [11]:

$$\dot{\gamma}(r) = \frac{2\Omega}{r^2\left(\frac{1}{R_1^2} - \frac{1}{R_2^2}\right)} \tag{1}$$

where r is the radius from the rotation axis of the rod ($R_1 \le r \le R_2$), Ω is angular frequency (rad/s), R_1 is the radius of the glass rod and R_2 is the inner radius of the glass tube. The calculated value of the shear rate varied from 598 s^{-1} at the surface of the glass rod to 724 s^{-1} at the tube wall. All shearing was performed at room temperature.

2.3. Shear viscosity measurement

The shear viscosities of the SF/SS blend solutions were measured using Rheometric Expansion System (ARES, Rheometric Scientific, US) as a function of shear rate (0.01–1000 s^{-1}). A cone and plate geometry were used to ensure a constant shear rate. The radius and angle of the cone were 50 mm and 0.04 rad, respectively. The measurement was conducted at room temperature.

2.4. Dynamic light scattering (DLS)

To measure the molecular size and distribution of SF and SS in aqueous solution before and after shearing, DLS analysis was conducted using a DLS spectrophotometer (DLS-7000, Otsuka Electronics, Japan). In order to prepare the solutions, the 5 wt% SF/SS blend solutions were sheared for 30 min; after shearing, the concentrations were diluted to 1 wt%. The concentration of the unsheared solution was also adjusted to 1 wt%. All solutions were kept at 4 °C until measurements were taken to prevent aggregation of SFs. Each solution was moved into a cell of 1 cm path length and an Argon laser was used as a light source. The measuring angle of the scattering was 90° and all measurements were conducted at room temperature. The hydrodynamic radius and distribution were calculated by analysis software.

2.5. Circular dichroism (CD)

The samples were prepared for CD analysis by the same method as described above for DLS measurements but the concentrations were adjusted to 0.05 wt% instead of 1 wt%. The CD spectra of the SF/SS blend solutions were obtained using a circular dichroism detector (J-715, Jasco, Japan) and the wavelength range was 190–250 nm with a resolution of 0.2 nm and an accumulation of 20 scans at a scanning rate of 50 nm/min. In order to estimate the β-sheet fraction of the solution, the normalized ellipticity at 217 nm was obtained by Eq. (2) [19,20].

$$f_\beta = \frac{[\theta]_{217}^{\exp} - [\theta]_{217}^{\mathrm{coil}}}{[\theta]_{217}^{\max} - [\theta]_{217}^{\mathrm{coil}}} \tag{2}$$

where f_β is the fraction of β-sheet, $[\theta]_{217}^{\exp}$ is the measured value of the ellipticity at 217 nm, $[\theta]_{217}^{\mathrm{coil}}$ is the ellipticity at 217 nm of a spectrum corresponding to SF's random coil conformation (minimum value among the results) and $[\theta]_{217}^{\max}$ is the maximum ellipticity value, which is expected for the sample with the highest β-sheet content.

2.6. FTIR spectroscopy

In order to obtain an SF/SS blend in a solid state, films were cast from unsheared and sheared solutions at 60 °C. The sheared solution was obtained from the supernatant of the residual solution after shearing for an hour. After the aggregates were retrieved, they were washed with distilled water and dried at 60 °C. These samples were also used in NMR and DSC analysis. FTIR spectra of the SF/SS blend films (approximately 10 μm thickness) and the aggregates were obtained using the Midac M series (USA) in a spectral region of 4000–400 cm^{-1} to determine the molecular conformations of SF/SS blends. For aggregates, the samples were measured by the KBr pellet method.

2.7. Solid-phase ^{13}C CP/MAS NMR

The β-sheet transition of SF was determined by ^{13}C NMR spectroscopy using a Soli/Micro-Imaging High Resolution NMR spectrometer (400 MHz, AVANCE 400 WB, DSX-400, Brücker, Germany) with a spin rate of 7 kHz. For sample preparation, the films and the aggregates were milled mechanically after soaking in liquid nitrogen.

2.8. Differential scanning calorimetry (DSC)

The thermal properties of an SF/SS blend were investigated using a Thermal Analysis Instrument (TA2910, TA Instrument, USA) at a scanning rate of 10 °C/min under nitrogen flow of 50 ml/min. The analysis was conducted in the temperature range of 100–300 °C.

3. Results and discussion

3.1. Solution properties of SF/SS blends

Fig. 1 shows the viscosity changes of SF/SS blend solutions with shear rate. The rheological behavior of the SF/SS blend solution was measured at 10% concentration as this concentration was a maximum for maintenance of homogeneity and stability of the solution for instrument sensitivity. As shown in Fig. 1, SF/SS solutions exhibit shear thinning behavior as expected. It has been reported that an aqueous SF solution shows shear thinning behavior with increasing shear rate like other common polymer solutions or melts [4,21–24].

As SS content increased in the solution, the shear viscosity was relatively higher at a low shear rate and sharply decreased with increasing shear rate. Eventually, at a high shear rate (more than 100 s^{-1}), the shear viscosities were almost the same regardless of the SS content. Higher shear viscosity with large SS content can be due to the naturally high viscous nature of SS. It is known that an SS solution shows faster gelation at room temperature than an SF solution of the same concentration, although the viscosity of the SS solution is difficult to measure due to the rapid gelation. Therefore, the SS might increase the entanglements or physical interactions of SF and SS chains in the blend solution by mainly forming hydrogen bonds.

We observed a rapid diminishment of the shear viscosity with increasing shear rate of an SF/SS solution containing high SS content. Generally, the shear thinning behavior can be explained by the loosening of entangled chains under shear. A rapid viscosity decrease can be caused by simultaneous fast loosening of the entanglement of both SF and SS chains, or SS compels the entangled SF chains to be loosened more quickly upon shearing. As mentioned previously, if some physical binding forces exist between SF and SS chains, SS can stretch the entangled SF chains under shear. Consequently, if SS coexists with SF, the SF chains can be more easily oriented in aqueous solution when relatively low shear force is applied.

DLS results show an interesting phenomenon in Fig. 2, which depicts the mean hydrodynamic radii (R_H) of components occupying major size distribution in SF/SS blend solutions. The small number of large R_H is assumed to be aggregates in the size distribution (data not shown). The R_H of SF in pure SF solution was about 10 nm before shearing and increased to about 20 nm after shearing. It might be because the sheared SF molecules cohered and formed bigger particles in the solution before precipitation. And it is considered as an intermediate state for complete crystallization with β-transition. On the other hand, the R_H value of an unsheared SF/SS blend solution decreased with increasing SS content. In the case of a sheared solution, the R_H values of the SF/SS solutions containing 10% and 20% SS were much lower than the R_H values before the shearing. Moreover, the R_H values of the sheared solutions were not significantly different from each other regardless of SS content (10–25%).

These results suggest that the bulkiness of SF particles (consisting of one or a few molecules) in a blend solution can be decreased by two factors: presence of SS and mechanical shearing, assuming that the main component of the blend solution is SF and

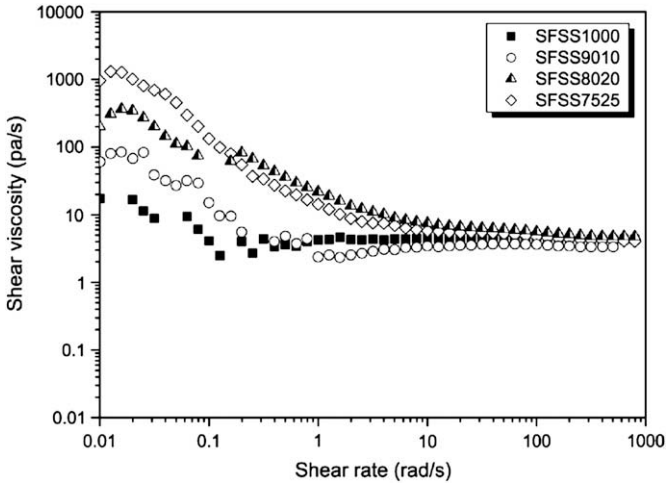

Fig. 1. Shear viscosities of SF/SS blend solutions with increasing shear rate.

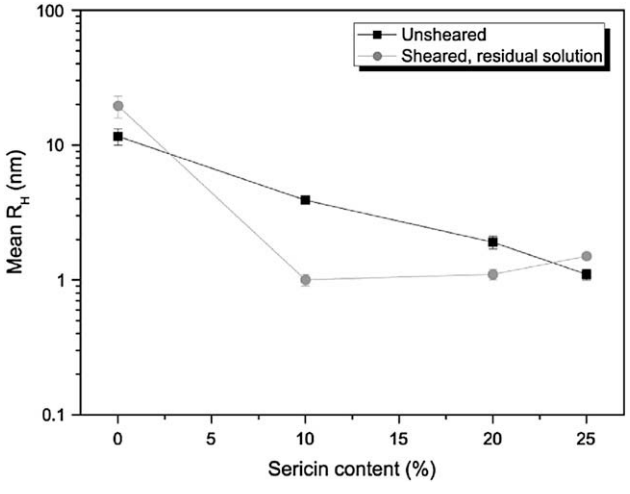

Fig. 2. Mean hydrodynamic radii of particles occupying major size distribution in SF/SS blend solutions.

the R_H of SS is not smaller than that of SF due to the difference in molecular weight. The fact that SF and SS molecules are not miscible with each other and exist separately in the blend should also be considered [13]. Before shearing, the diminishment of the R_H might be due to two reasons. One is the dehydration from SS surrounding SF molecules in aqueous solution. There is relatively high affinity between water molecules and SS because SS, which contains a lot of hydrophilic amino acids such as serine and threonine is much more hydrophilic than SF. Consequently, the SF molecules can be entangled more compactly in the aqueous state in the presence of SS. The other is due to the change of average R_H with the increase of SS content based on the fact that the SS' R_H is smaller than that of SF. However, it is impossible to measure the R_H of SS because the SS solution turned to gel during the dialysis and the higher R_H value of SFSS7525 after shearing, compared with SFSS9010 and SFSS8020, might mean that the decrease of R_H with the SS content is not wholly dependent on the SF/SS composition.

When shear stress was applied, the effect of SS was more predominant. Above only 10% SS content, the mean R_H value dropped considerably to 1–2 nm (limit of measurable R_H value) when compared with that of the unsheared solution. The decrease of the R_H value under shear might be due to the aligning effect of SS. In the presence of SS, SF molecules were more stretched along the shear direction compared with pure SF solution under the same shear rate. However, the R_H of pure SF solution was rather increased. This may be explained by the following: there might be a critical size to form an aggregate by shear and the SF molecules, which did not reach the critical size, could not exist in soluble state in the residual solution. By contrast, more compactly entangled molecules exist in the SF/SS solution and this can give a high opportunity to form β-sheet aggregation of SF by shear.

3.2. Formation of aggregates under shear

It is generally believed that an aggregate of SF formed by shear is caused by a β-sheet transition and crystallization of SF. In the regeneration process, SS may largely affect the crystallization of SF under shear stress [5]. In this study, the amount of aggregates of SF formed by shearing was determined indirectly by measuring the concentration of the residual solution with varying SF/SS blend ratios and shearing time (0–2 h). After shearing, the residual solution was retrieved and centrifuged to remove debris. Then the concentration of the supernatant was measured using a moisture analyzer (MB35, Ohaus, US).

Fig. 3 shows the concentrations of the residual solutions after shearing with time. The lower the concentration of the residual solution, the larger the amount of SF aggregates formed. As shown in Fig. 3, the concentrations of the residual SF/SS blend solutions (SFSS9010 and SFSS8020) were markedly decreased when a proper amount of SS (ca. 10–20%) was blended. On the other hand, the concentrations of pure SF and a higher SS-containing blend solution (SFSS7525) were relatively higher for the same shear time. Moreover, the SFSS9010 and SFSS8020 samples differed from the pure SF in that the low concentrations were not significantly changed after 1.5 h and were constantly maintained afterwards. This indicates that most of the SF aggregates were formed in SF/SS blend solutions after 1.5 h of shearing.

Assuming that the rate of aggregate formation is related to the crystallization rate, the rate of β-sheet crystal formation of SF was constant under shear. This result agrees well with other reports which have stated that the kinetics of SF crystallization is proportionally linear with time [23–26]. However, when the rate constants (slopes of straight lines) were compared, the samples containing 10–20% SS (SFSS9010 and SFSS8020) showed faster crystallization (β-sheet transition). Therefore, the SS can accelerate

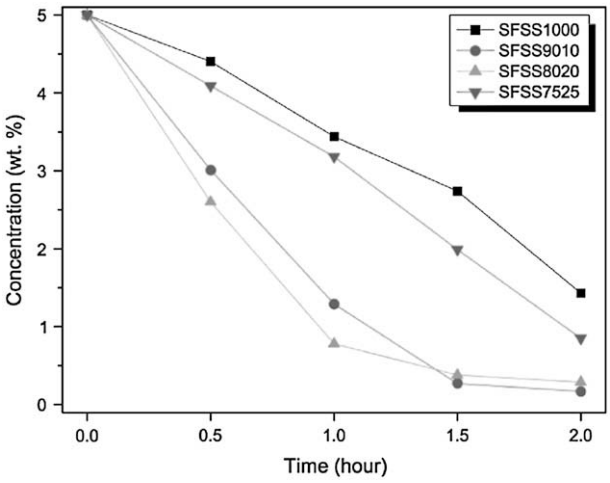

Fig. 3. Concentration changes of SF/SS blend solutions under shear with time.

the β-sheet transition of SF in an SF/SS blend solution under shear and the degree of acceleration seems to be dependent on the amount of SS in the blend. The highest acceleration was achieved for SF/SS solutions containing 10–20% SS. The effect of acceleration (faster crystallization) will be further discussed in Section 3.3.

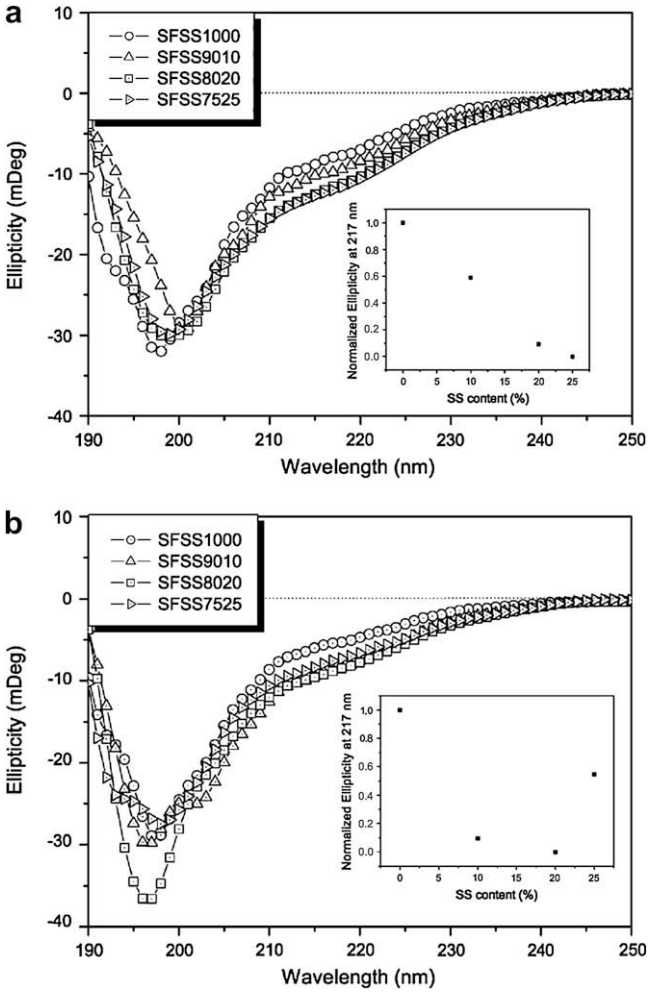

Fig. 4. CD spectra of SF/SS blend solutions: unsheared (a) and sheared for 30 min (b). In the box, normalized ellipticity at 217 nm of each figure is plotted against SS content.

3.3. Conformational analysis

To investigate the conformational transition of SF/SS blends, the secondary structures of SF and SS were analyzed. Specifically, the conformation in aqueous state was measured by CD because it is important to confirm the increase in crystallization rate and amount of aggregates due to β-sheet transition of SF in solution. Generally, it is well known that both SF and SS have random coil conformations in aqueous solution. Fig. 4(a) depicts the CD spectra of the unsheared SF/SS blend solutions. The random coil conformation was observed for the unsheared solutions and the spectra of the residual solutions after shearing also dominantly exhibited randomly coiled structures (Fig. 4(b)). This result corresponds with those of previous reports [19,20].

On the other hand, when the normalized ellipticity at 217 nm (which can estimate the β-sheet fraction) was plotted against SS content, an interesting result was obtained as shown by the figures in the box of Fig. 4. The normalized ellipticity constantly decreased with increasing SS content before shearing, while those of the residual solutions of SFSS9010 and SFSS8020 were relatively lowered compared with the other solutions. Yang et al. reported that a low normalized ellipticity at 217 nm indicates a relatively large content of β-sheet conformation of SF [19]. Therefore, our result indicates that the β-sheet transition can occur more easily when SS exists with SF in the blend solution and the acceleration of the β-transition occurs with proper amounts of SS under shear stress.

Qualitative analyses were conducted for solidified SF/SS blends using FTIR and NMR spectroscopy in order to examine the effect of SS on conformational characteristics and transition of SF. Fig. 5 depicts FTIR spectra in the range of 1800–1200 cm^{-1} for SF/SS blend films cast from unsheared and sheared solutions. For films cast from unsheared solutions (Fig. 5(a)), all samples showed similar spectra in which amide I–III bands, which are used for determining the secondary structure of proteins, appeared at around 1650, 1540 and 1230 cm^{-1}, respectively. These amide band positions are attributed to the randomly coiled structure of SF regardless of the SS content. However, in aggregates formed by shearing (Fig. 5(b)), amide I and II bands shifted to lower wave numbers, 1630 and 1520 cm^{-1}, respectively, with a shoulder peak at 1260 cm^{-1}. Such amide band locations correspond to a typical FTIR spectrum of crystallized SF possessing β-sheet structure. This is strong evidence that the formation of aggregates under shear stress originates from the β-sheet transition of SF whether or not SS is present in the blends.

On the other hand, for films cast from the residual solution after shearing, the film cast from pure SF solution (SFSS1000) exhibited amide bands corresponding to random coil conformation while the conformations of the SS-containing films were β-sheet, as shown in Fig. 5(c). Therefore, it can be said that the conformational transition is favorable and the composition of β-sheet structure is highest when the SS content is 10% in SF/SS blends.

As a result, shear stress is essential in order to obtain an enhancement of β-sheet transition of SF by SS. Furthermore, we can assume that the presence of SS can be positive for complete β-sheet crystallization of SF. The β-sheet transition of the SS-containing films of residual solution, however, is somewhat discordant with our previous CD result. This could be explained by the different states the samples are in for FTIR and CD analyses. Although the SF chains are randomly coiled after the SF molecules are compacted by SS under shear stress, it can easily undergo β-sheet transition and crystallization during the solidification process due to an increase in concentration with water evaporation.

Solid-phase ^{13}C NMR spectroscopy, which can provide more reliable information about secondary structure of SF was carried out for SF/SS blend films. Fig. 6 shows ^{13}C NMR spectra attributed to an alanine β carbon of SF. For the unsheared solutions, the peaks appeared around 17 ppm, corresponding to a random coil conformation (Fig. 6(a)). On the other hand, in Fig. 6(b), the aggregates exhibited main peaks at 22 ppm and a shoulder at 17 ppm regardless of SS content. This means that the β-sheet transition of SF occurs in all the aggregate samples after shearing but some portions remain as random coil conformation. Here, it should be noted that the results only represent the characteristic conformation of SF and not of SS. This is because the corresponding peak of SS at 19 ppm, which has been confirmed by our previous report [5], hardly overlaps with those of SF at 17 and 22 ppm and the weight portion of SS is not more than 25% in the blend.

Fig. 6(c) shows ^{13}C NMR spectra of the blend films cast from the residual solutions after shearing. In addition to the random coil conformation of SF, the β-sheet structure, on the whole, developed

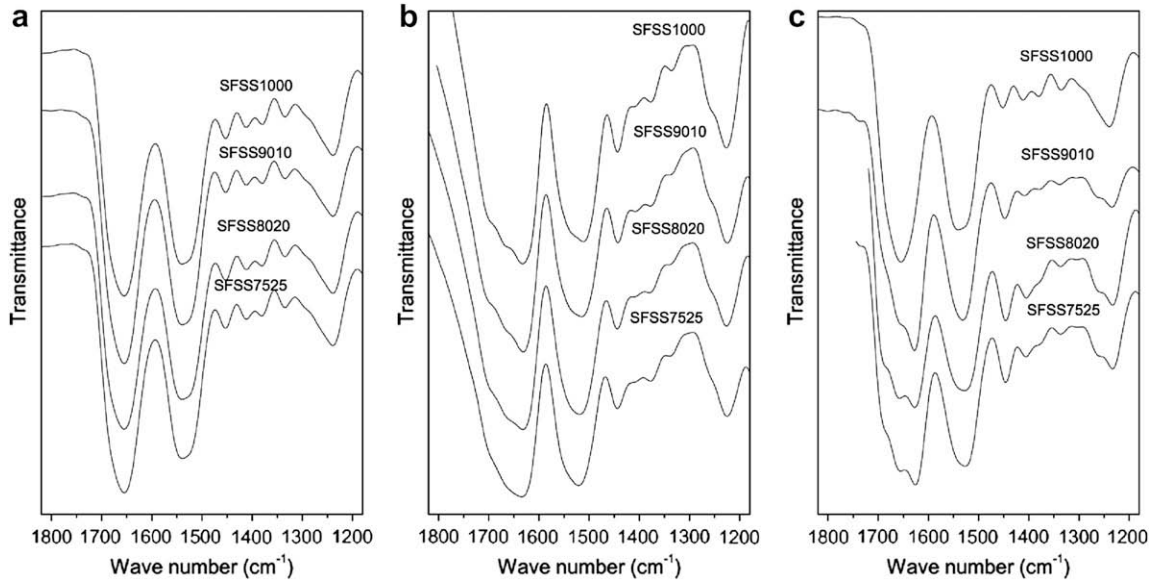

Fig. 5. FTIR spectra of SF/SS blend films of various blend ratios cast from unsheared SF/SS solution (a), of aggregates (b) and from residual solution after shearing (c).

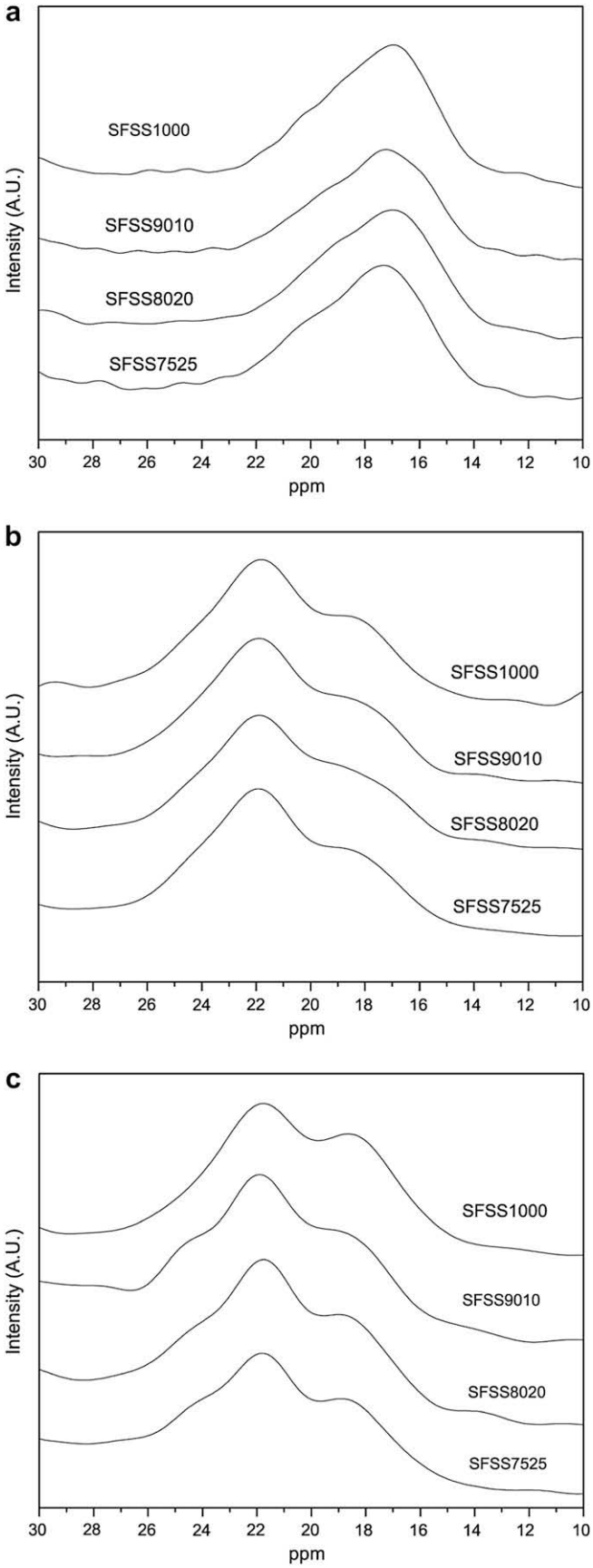

Fig. 6. Solid-phase ^{13}C CP/MAS NMR spectra of SF/SS blend films of various blend ratios cast from unsheared SF/SS solution (a), of aggregates (b) and from residual solution after shearing (c).

in all the samples, even in pure SF film. The SFSS1000 sample exhibited relatively low β-sheet content because the intensity of a sub shoulder peak at 17 ppm (attributed to random coil conformation) was higher than the other SS-containing samples. It is interesting that a shoulder peak appeared at 24 ppm, corresponding to SF's β-sheet conformation, for the SFSS9010 sample. This indicates that a proper amount of SS can affect the β-crystallization of SF, and SS content of 10% is most appropriate for developing β-sheet structure of SF under shear stress. We confirmed that the ^{13}C NMR results are exactly coincident with FTIR results on conformational changes of SF/SS blends under shearing.

3.4. Thermal behavior

Fig. 7 shows thermal behavior of SF/SS blend films measured by DSC. The films, which were prepared from the unsheared SF/SS blend solutions, exhibited typical thermograms of regenerated SF prior to recrystallization. The regenerated SF (without any crystallization treatment) usually presents a random coil conformation of amorphous state, which was confirmed by FTIR and ^{13}C NMR results. In this study, the glass transition was observed at around 180 °C and its exothermic peak of crystallization appeared in the range of 217–220 °C, while any particular thermal transition of SS was not observed in the temperature range of 150–250 °C. Thus, it is clear that the crystallization of SF due to β-sheet transition did not occur in SF/SS blend films prepared from unsheared solutions. However, the crystallization peak shifted to higher temperature with an increase of SS content. This indicates that the SS may affect the crystallization of SF. If physical interactions exist between SF and SS molecules at the interface, these can restrict the chain mobility of SF and hinder the regular packing needed for crystallization, resulting in a higher crystallization temperature of SF in the blend. We propose that hydrogen bonding is occurring and that these molecular interactions (between SF and SS as well as between SF chains) can affect the crystallization process of SF. The SFSS7525 sample showed a somewhat sharper peak and higher crystallization temperature.

However, for the aggregates (Fig. 7(b)), neither crystallization nor glass transition temperature was observed as expected. This is because the aggregates, which were prepared under shear stress, consist of β-sheet crystalline structure with a small amorphous region. The thermal behavior of the aggregates is strongly supported by the FTIR and ^{13}C NMR results. The blend films cast from the sheared residual solution also exhibited the same tendency in thermal behavior as previous conformational analysis results. The sheared pure SF sample (SFSS1000) in Fig. 7(c) showed a similar thermogram to the unsheared sample in Fig. 7(a). Therefore, the SF, which remained in the residual solution after shearing, is in an amorphous state of random coil structure like unsheared SF and it is crystallized during the DSC measurement. However, for SS-containing blends in Fig. 7(c), the samples exhibited thermal behavior similar to the crystallized SF aggregates in Fig. 7(b). Therefore, it is obvious that the SS significantly affects the thermal transition of SF in SF/SS blends prepared under shear stress. These DSC results are completely coincident with previous FTIR and ^{13}C NMR results for the effect of SS on the β-sheet structural transition and crystallization of SF in either shearing or non-shearing conditions.

3.5. Role of SS in crystallization

According to our results, a mechanism of acceleration and perfection of SF crystallization under shear can be proposed as shown in Fig. 8. First of all, we suppose the micellar structure of SF, which can be formed in aqueous solution due to their amphiphilic nature according to previous reports by Jin et al. and Ha et al.

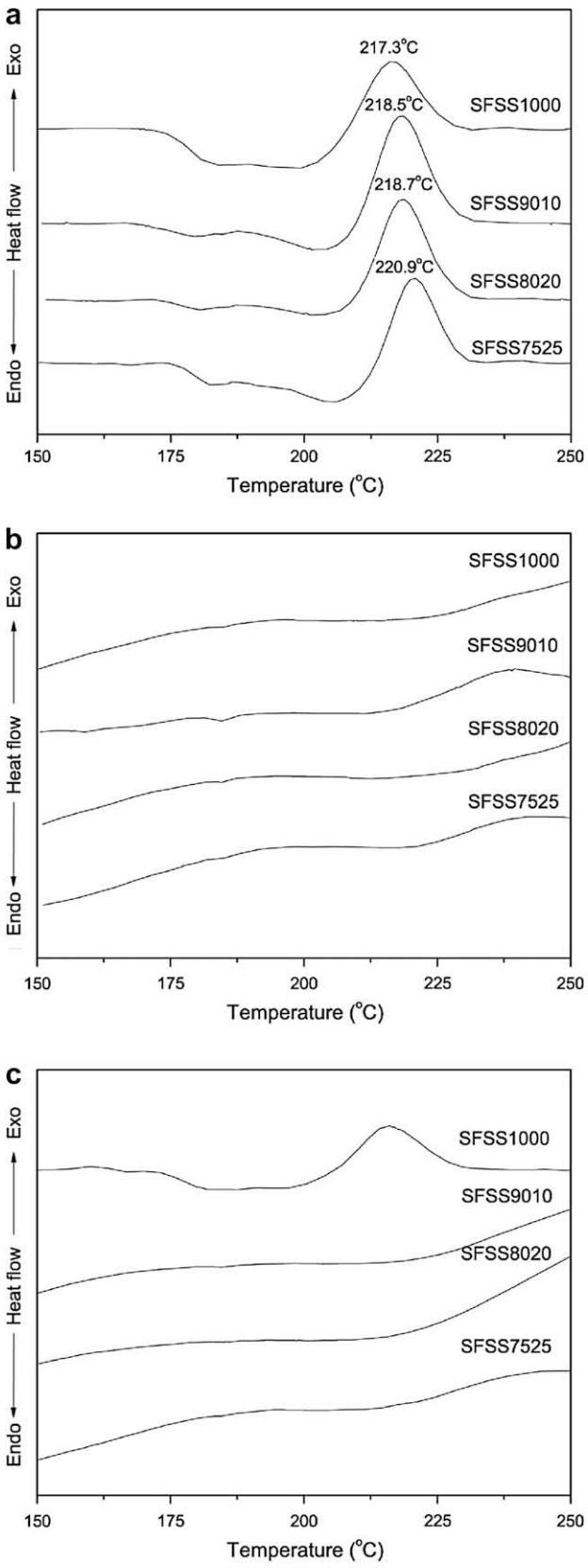

Fig. 7. DSC thermograms of SF/SS blend films of various blend ratios cast from unsheared SF/SS solution (a), of aggregates (b) and from residual solution after shearing (c).

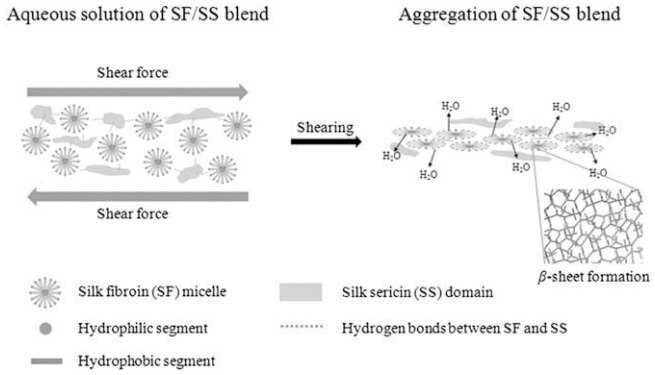

Fig. 8. Schematic diagram of the crystallization process of SF in SF/SS blend under shearing conditions.

[27,28] although this article does not directly deal with neither provide an evidence of the micellar structure of SF. And fundamentally, SF can form a crystalline structure of β-sheet conformation by shearing. When shear force is applied to the SF solution or gel, the SF tends to be stretched in the direction of shear. Then, the inter- or intra-molecular distance becomes very close and the β-sheet transition and crystallization easily occur by forming strong hydrogen bonds between hydrophobic segments, mainly composed of GAGAGS peptide sequences in SF molecules.

When SS is blended with SF in aqueous solution, hydrophilic SS molecules are located at the exterior of SF micelles due to their immiscibility in aqueous solution. Lee reported that SF and SS molecules formed their own separate domains in aqueous SF/SS solution [13]. Accordingly, the SS extract water molecules in the SF micelle due to its relatively high hydrophilicity and these results in the diminishment of the micelle size of SF due to an increase of SF chain packing density. Nevertheless, such an effect of SS is probably not sufficient for the enhancement of the β-sheet transition and crystallization rate.

However, when shear stress is applied, SS plays a critical role in the SF/SS blend by inducing the β-sheet structural transition of SF. Upon shearing, the SF micelles become elongated by frictional force between the molecules. When SS is blended with SF, the frictional force can be increased by hydrogen bonding at the interfaces. And the stretched SF chains are more densely packed against SS compared with the SF chains in pure SF solution. Subsequently, the densely packed chains of SF aggregates yield the β-sheet structure predominantly and crystallization occurs more easily. Therefore, SS can enhance and accelerate the β-sheet crystalline transition in SF/SS blends.

4. Conclusion

In this study, we elucidated the effect of SS on the β-sheet transition and crystallization of SF under shear stress. This investigation continues from our previous work in which the improvement of the crystallinity and mechanical properties of regenerated silk were realized using a regenerated silk filament fabricated from partially degummed silk cocoons (remaining sericin content of ca. 10%) [5]. We concluded that such a phenomenon is probably due to the existence of SS because the SS can contribute to an acceleration and perfection of SF crystalline structure in the regenerated filament when shear stress is applied during fiber formation. Furthermore, it was hypothesized that such a result is mainly due to the formation of hydrogen bonds between SF and SS. Consequently, we confirmed that the SS significantly affects the acceleration of β-sheet structural transition of SF under shear. And it was found that shear-induced crystallization can be enhanced with the SS when the SF is blended with a proper amount of SS.

Acknowledgment

This work was supported by the Korea Research Foundation Grant funded by the Korean Government (MOEHRD) (KRF-2007-313-D00943) and the SRC/ERC Program of MOST/KOSEF (R11-2005-065) of the Korea Science and Engineering Foundation (KOSEF).

References

[1] Kang GD, Lee KH, Ki CS, Park YH. Fiber Polym 2004;5(3):234–8.
[2] Fini M, Motta A, Torricelli P, Giavaresi G, Aldini NN, Tschon M, et al. Biomaterials 2005;26:3527–36.
[3] Kweon HY, Um IC, Park YH. Polymer 2000;41(20):7361–7.
[4] Um IC, Ki CS, Kweon HY, Lee KG, Ihm DW, Park YH. Int J Biol Macromol 2004;34:107–19.
[5] Ki CS, Kim JW, Oh HJ, Lee KH, Park YH. Int J Biol Macromol 2007;41:346–53.
[6] Freddi G, Pessina G, Tsukada M. Int J Biol Macromol 1999;24:251–63.
[7] Ki CS, Kim JW, Hyun JH, Lee KH, Hattori M, Rah DK, et al. J Appl Polym Sci 2007;106:3922–8.
[8] Kweon HY, Um IC, Park YH. Polymer 2001;42(15):6651–6.
[9] Roh DH, Kang SY, Kim JY, Kwon YB, Kweon HY, Lee KG, et al. J Mater Sci Mater Med 2006;17:547–52.
[10] Huang T, Ren P, Huo B. J Appl Polym Sci 2007;106:4054–9.
[11] Ohgo K, Bagusat F, Asakura T, Scheler U. J Am Chem Soc 2008;130:4182–6.
[12] Roessle M, Panine P, Urban VS, Riekel C. Biopolymers 2004;74:316–27.
[13] Lee KH. Macromol Rapid Commun 2004;25:1792–6.
[14] Garcia-Fuentes M, Giger E, Meinel L, Merkle HP. Biomaterials 2008;29(6):633–42.
[15] Tsukada M, Goto Y, Minoura N. J Seric Sci Jpn 1990;59(5):325–30.
[16] Yamada H, Nakao H, Takasu Y, Tsubouchi K. Mater Sci Eng C Bio S 2001;14:41–6.
[17] Takasu Y, Yamada H, Tsubouchi K. J Insect Biotechnol Sericol 2002;71:151–6.
[18] Teramoto H, Miyazawa M. Biomacromolecules 2005;6:2049–57.
[19] Yang Y, Shao Z, Chen X, Zhou P. Biomacromolecules 2004;5:773–9.
[20] Li XG, Wu LY, Huang MR, Shao HL, Hu XC. Biopolymers 2008;89(6):497–505.
[21] Holland C, Terry AE, Porter D, Vollrath F. Nature 2006;5:870–4.
[22] Raghu A, Somashekar R, Sharath A. J Polym Sci Polym Phys 2007;45:2555–62.
[23] Hossain KS, Ohyama E, Ochi A, Magoshi J, Nemoto N. J Phys Chem 2003;107:8066–73.
[24] Ochi A, Hossain KS, Magoshi J, Nemoto N. Biomacromolecules 2002;3(6):1187–96.
[25] Hossain KS, Ochi A, Ohyama E, Magoshi J, Nemoto N. Biomacromolecules 2003;4(2):350–9.
[26] Chen X, Shao Z, Knight DP, Vollrath F. Proteins 2007;68:223–31.
[27] Jin HJ, Kaplan DL. Nature 2003;424:1057–61.
[28] Ha SW, Gracz HS, Tonelli AE, Hudson SM. Biomacromolecules 2005;6(5):2563–9.